IAGA WG 1.2 on Electromagnetic Induction in the Earth
20th Workshop Abstract
Giza, Egypt , September 18-24, 2010

Magnetotelluric and xenolith constraints on the thermal and chemical lithospheric-mantle structure of the Kaapvaal Craton and Rehoboth Terrane, southern Africa

Mark R. Muller, Javier Fullea and Alan G. Jones
Dublin Institute for Advanced Studies, Dublin, Ireland

SUMMARY

A 1400 km-long, 2-D magnetotelluric (MT) profile across the Archaean Kaapvaal Craton and the Proterozoic Rehoboth Terrane reveals significant lateral heterogeneity in the electrical resistivity structure of the southern African lithosphere. Comparison of the present-day lithospheric-mantle structure, well defined in 2-D smooth inversion models of the MT data, with the palaeo-structure revealed by mantle xenoliths from the Kimberley and Gibeon kimberlite fields, suggests that the physical, thermal and chemical lithospheric-mantle structure of both the Kaapvaal Craton and the Rehoboth Terrane may have been substantially and relatively rapidly modified by the thermalism and magmatism associated with Mesozoic kimberlite volcanism. Such modifications would generate a significant isostatic uplift/subsidence response, with predictable changes in surface elevation, which can be tested against the geological record of deposition and erosion since ~100 Ma. Testing whether such modifications are plausible forms one focus of this research. In a second area of interest, we aim to derive 1-D models of the chemical, physical and petrological properties of the Kaapvaal and Rehoboth lithospheres that are consistent with observed MT responses. Using the LitMod approach, we compute self-consistent models of the petrology of the lithospheric- and sublithospheric-mantle as a function of chemical composition (including water content), temperature and pressure, and derive physical properties of the models – density and electrical resistivity – that are tested against observables at surface – the MT response, as well as surface heat-flow and elevation. Our preliminary results establish the efficacy of the modelling approach and provide clear indications of the model sensitivities to chemical composition, lithospheric thickness and water content variations. Our paper will present more detailed results from these ongoing lines of research.

Keywords: Kaapvaal, Rehoboth, magnetotellurics, xenoliths, lithospheric-mantle

INTRODUCTION

A 1400 km-long, 2-D magnetotelluric (MT) profile across the Archaean Kaapvaal Craton, the Proterozoic Rehoboth Terrane and the Late Proterozoic/Early Phanerozoic Ghanzi-Chobe/Damara Belt (Fig. 1) allowed estimates to be made of the lithospheric thickness and conductive geotherm for each terrane (Fig. 2) (Muller *et al*., 2009). Differences are apparent between the present-day (hotter) lithospheric geotherm inferred from the resistivity model for the Rehoboth Terrane and the (cooler) palaeo-geotherm inferred from Mesozoic kimberlitic xenolith pressure-temperature (P-T) arrays (Bell *et al*., 2003; Grütter and Moore, 2003; Boyd *et al*., 2004; Appleyard *et al*., 2007). A compilation of xenocryst Cr/Ca-in-pyrope barometry observations (Muller *et al*., 2009) indicate a depth to the base of the depleted mantle some 60 km shallower than the present-day lithospheric thickness (Fig. 2). Reconciling both observations suggests a history for the Rehoboth Terrane in which an originally thicker lithosphere was rapidly heated, thinned (perhaps by ~40 km) and refertilised upwards from its base at an early stage of Mesozoic thermalism (Bell *et al*., 2003; Muller *et al*., 2009). A similar fate has also been inferred for the Kaapvaal Craton. A hotter geotherm was established, and the lower lithospheric mantle refertilised, in the period between the eruption of Group 2 (143 – 117 Ma) and Group 1 kimberlites (108 – 74 Ma) (Kobussen *et al*., 2008). Both the Rehoboth and Kaapvaal cases suggest that thermal and chemical disruption of the lithosphere during the thermalism and magmatism associated with kimberlite genesis is possible over relatively short periods of time, perhaps of the order of ~50 Ma.

RESEARCH OBJECTIVES AND APPROACH

In our first area of investigation we test 1-D models that describe our current understanding of the present-day chemical composition and physical structure of the Kaapvaal and Rehoboth lithospheres, by deriving their associated electrical resistivities in a petrophysically self-consistent way, and comparing their predicted MT responses against observed responses. Secondly we aim to test the plausibility of the lithospheric-mantle modifications described above (thinning and chemical refertilisation), given that they would be associated with significant, time-varying isostatic uplift and subsidence responses, with predictable changes in surface elevation.

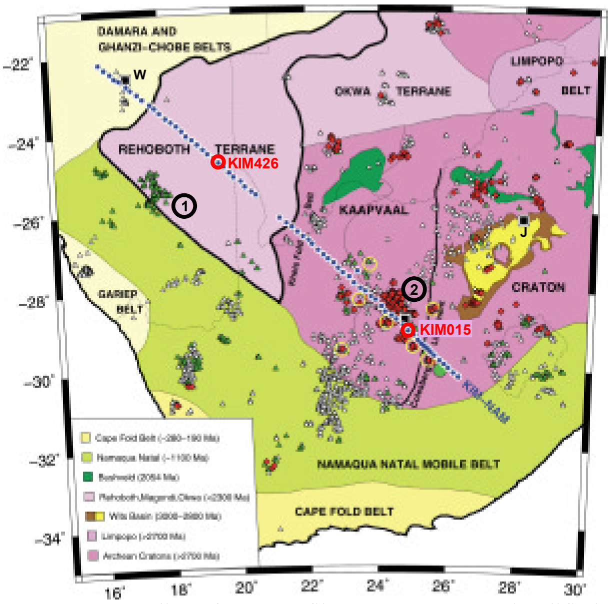

Figure 1. Locality of MT profile KIM-NAM on simplified tectonic map of southern Africa. Shown are MT sites (blue dots) and kimberlite occurrences (red diamonds = known diamondiferous, green triangles = known non-diamondiferous, white triangles = unknown or unspecified in databases). Annotated kimberlite fields: (1) Gibeon, (2) Kimberley. Specific kimberlites providing Cr/Ca-in-pyrope barometry observations (Fig. 2) are shown by yellow circles. Localities of MT sites KIM426 and KIM015 (Fig. 3) are shown by red circles. Major cities (black squares) annotated: Johannesburg (J), Windhoek (W). Sources of kimberlite data: South African Council for Geoscience numerical database; Jelsma et al. (2004); Faure (2006). Terrane boundaries courtesy S.J. Webb, University of the Witwatersrand, based on the magnetic field image of southern Africa.

Our approach, in tackling both objectives, is built within the self-consistent thermodynamic/geophysical framework of LitMod (Afonso *et al.*, 2008; Fullea *et al.*, 2009), where all thermo-petrophysical properties in the mantle are functions of the Gibbs free energy of the stable mineral assemblages (Connolly, 2005). The main advantage of the approach is that essential parameters describing the mantle structure (e.g., density, seismic velocity and electrical resistivity) are obtained consistently as a function of temperature, pressure and chemical composition, rather than being imposed independently or on an *ad hoc* basis.

MT resposnse modelling. Modal compositions for olivine, clinopyroxene, orthopyroxene, spinel and garnet are computed given an input layered chemical model of the lithosphere. Resistivities for individual minerals are derived from extant pressure- and temperature-dependent laboratory measurements. The bulk-rock resistivity is determined using Hashin-Shtrikman bounds theory for the mixing of multi-phase materials (Jones *et al.*, 2009). One-dimensional forward modelling of the bulk rock resistivities produces MT responses that are compared against observations. Both dry and wet mantle compositions are examined.

Surface elevation modelling. Self-consistent pressure- and temperature-dependant densities are computed for 1-D lithospheric models of the chemical composition and thickness of the lithosphere, before and after magmatic/thermal modification. The surface elevation changes predicted from these models, assuming local isostatic compensation, can be tested against the geological record of erosion (uplift) and deposition (subsidence) since ~100 Ma.

Table 1. Representative chemical compositions of the mantle used for LitMod modelling. Average Kaapvaal compositions, from Afonso *et al.* (2008), are used for the lithospheric-mantle. The primitive upper mantle (PUM) composition of McDonough and Sun (1995) is used for the sub-lithospheric mantle. The Mg# shown refers to that for olivine.

	Aver. Kaapvaal Harzburg.	Aver. Kaapvaal low-T Lherzolite	Aver. Kaapvaal high-T Lherzolite	PUM M&S95
SiO_2	45.9	46.5	44.4	45
TiO_2	0.05	0.05	0.17	0.2
Al_2O_3	1.3	1.4	1.75	4.5
Cr_2O_3	0.34	0.34	0.3	0.38
FeO	6.0	6.6	8.1	8.1
MnO	0.1	0.1	0.12	0.14
MgO	45.5	43.8	43.4	37.8
CaO	0.5	0.86	1.27	3.6
Na_2O	0.07	0.1	0.12	0.36
NiO	0.28	0.29	0.26	0.25
Mg#	93.1	92.2	90.5	89.3
Cr/(Cr+Al)	0.27	0.14	0.1	0.05

PRELIMINARY RESULTS

Preliminary tests and results based on nominal “representative” chemical compositions (Table 1) establish firstly the efficacy of the modelling approach. Secondly they provide an indication of the model sensitivities to variations in chemical composition, lithospheric thickness and water content, for the case of the modelled MT responses (Fig. 3) and for the surface elevation (isostatic) response to lithospheric modification (Fig. 4).

CONCLUSIONS

While the difficulty in matching the observed MT responses with a completely dry mantle structure is noted here (Fig. 3), particularly for the Rehoboth Terrane (the predicted apparent resistivities are too high), no definitive conclusions can be drawn yet from our preliminary results. Model space has yet to be fully explored – for example, the wet mantle model is wet everywhere, and the effect of introducing varying concentrations of water into different parts of the lithospheric-mantle needs to be evaluated, as does the effects of anisotropy caused by H^+ diffusion. New constraints on the water contents of Kaapvaal Craton xenoliths (e.g., Peslier, 2009) must also be taken into account.

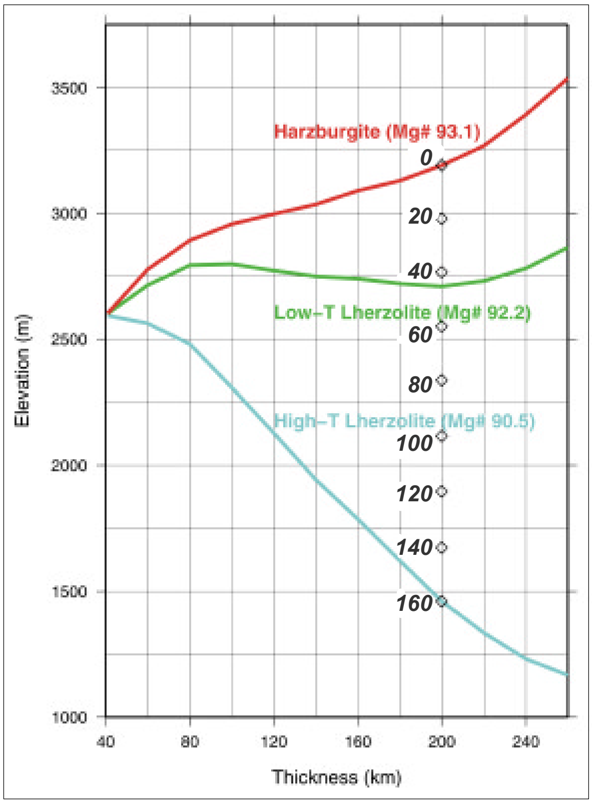

Figure 4. Modelled surface elevation versus lithospheric thickness curves for three different lithospheric-mantle compositions (Table 1) (red, green, blue lines). Crustal thickness is 40 km. Diamond symbols show the surface elevation response that results from replacing the lower part of a harzburgitic lithosphere (Mg# = 93.1), of 200 km thickness, with a layer of more fertile lherzolite (Mg# = 90.5). Thickness of the lower lherzolitic layer is as annotated.

The predicted steady-state response to both the thinning and the refertilisation of an initial harzburgitic lithospheric-mantle is subsidence of the order of several hundreds of meters (for each mechanism) (Fig. 4). In the case of intermediate levels of mantle depletion (Mg# = 92.2, Fig. 4), more appropriate for the Rehoboth lithosphere, the response to lithospheric thickness change is surprisingly subdued. Our initial results will be developed to incorporate the transient thermal effect of lithospheric thinning, which will manifest itself initially as heating and uplift, followed by a cooling (and subsidence) back to the steady-state geotherm defined by the final lithospheric thickness. The combined effect of all three mechanisms (thinning, refertilisation and transient thermal) is to be assessed with respect to available information about: (i) the preservation of the Karoo Supergroup (330–145 Ma) that predates kimberlite volcanism, for example, in the Aranos basin of the Rehoboth Terrane (e.g., Tankard *et al.*, 1982; Wanke, 2000) and (ii) deposition of the Kalahari basin sediments (<65 Ma) (e.g., Haddon, 2005) that post-date kimberlite volcanism. Our paper will present the results of these ongoing lines of research.

REFERENCES

Afonso, J.C. *et al.*, 2008. Integrated geophysical-petrological modeling of the lithosphere and sublithospheric upper mantle: Methodology and applications. Geochemistry, Geophysics, Geosystems, 9, Q05008, doi: 10.1029/2007GC001834.

Appleyard, C.M. *et al.*, 2007. Petrology and geochemistry of eclogite xenoliths from the Rietfontein kimberlite, Northern Cape, South Africa. Contributions to Mineralogy and Petrology, 154, 309-333.

Bell, D.R. *et al.*, 2003. Mesozoic thermal evolution of the southern African mantle lithosphere. Lithos, 71, 273-287.

Boyd, F.R. *et al.*, 2004. Garnet lherzolites from Louwrensia, Namibia: bulk composition and P/T relations. Lithos, 77, 573-592.

Connolly, J.A.D., 2005. Computation of phase equilibria by linear programming: a tool for geodynamic modeling and its application to subduction zone decarbonisation. Earth and Planetary Science Letters, 236, 524-541.

Faure, S., 2006. World Kimberlites and Lamproites CONSOREM Database (Version 2006-1). Consortium de Recherche en Exploration Minérale, Université du Québec à Montréal, www.consorem.ca.

Fullea, J. *et al.*, 2009. LitMod3D: An interactive 3-D software to model the thermal, compositional, density, seismological, and rheological structure of the lithosphere and sublithospheric upper mantle. Geochemistry, Geophysics, Geosystems, 10, Q08019, doi: 10.1029/2009GC002391.

Grütter, H., Moore, R., 2003. Pyroxene geotherms revisited – an empirical approach based on Canadian xenoliths. Extended Abstract, 8th International Kimberlite Conference, Canada.

Haddon, G.I., 2005. The Sub-Kalahari Geology and Tectonic Evolution of the Kalahari Basin, Southern Africa. Unpublished Ph.D. thesis, University of the Witwatersrand, Johannesburg.

Jelsma, H.A. *et al.*, 2004. Preferential distribution along transcontinental corridors of kimberlites and related rocks of Southern Africa. South African Journal of Geology, 107, 301-324.

Hashin, Z., Shtrikman, S., 1963. A variational approach to the theory of the elastic behaviour of multiphase materials. Journal of the Mechanics and Physics of Solids 11, 12–140.

Jones, A.G. *et al.*, 2009. Velocity–conductivity relationships for mantle mineral assemblages in Archean cratonic lithosphere based on a review of laboratory data and Hashin–Shtrikman extremal bounds. Lithos, 109, 131-143.

Kobussen, A.F. *et al*., 2008. Ghosts of lithospheres past: Imaging an evolving lithospheric mantle in Southern Africa. Geology, 36, 515-518.

McDonough, W.F., Sun, S., 1995. The composition of the Earth. Chemical Geology, 120, 223-253.

Muller, M.R. *et al*., 2009. Lithospheric structure, evolution and diamond prospectivity of the Rehoboth Terrane and western Kaapvaal Craton, southern Africa: constraints from broadband magnetotellurics. Lithos, 112S, 93-105.

Peslier, A.H., 2009. A review of water contents of nominally anhydrous natural minerals in the mantles of Earth, Mars and the Moon. Lithos, doi: 10.1016/j.jvolgeores.2009.10.006.

Pollack, H.N., Chapman, D.S., 1977. On the regional variation of heat flow, geotherms, and lithospheric thickness. Tectonophysics, 38, 279-296.

Rodi, W., Mackie, R.L., 2001. Nonlinear conjugate gradients algorithm for 2-D magnetotelluric inversion. Geophysics, 66, 174-187.

Tankard, A.J. *et al*., 1982. Crustal Evolution of Southern Africa. Springer, Berlin, pp. 523.

Wanke, A., 2000. Karoo-Etendeka Unconformities in NW Namibia and their Tectonic Implications. Unpublished Ph.D. thesis, Julius-Maximilians University, Würzburg.

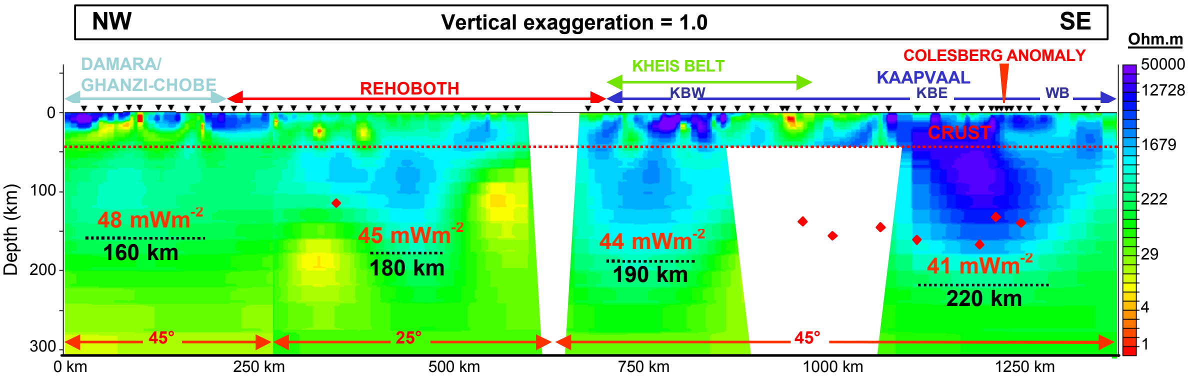

Figure 2. Composite electrical resistivity model for Profile KIM-NAM derived from 2-D smooth inversion (using Rodi and Mackie, 2001) of decomposed MT data (decomposition strike azimuth annotated) (from Muller *et al*., 2009). Model is blanked where unconstrained. Interpreted depths to the base of the "thermal" lithosphere shown where well constrained (dashed black lines), with inferred conductive geotherms (red text) (using Pollack and Chapman, 1977). Red diamond symbols show depth to base of highly-depleted mantle, from xenocryst Cr/Ca-in-pyrope barometry observations (Muller *et al*., 2009) for kimberlites shown in Fig. 1.

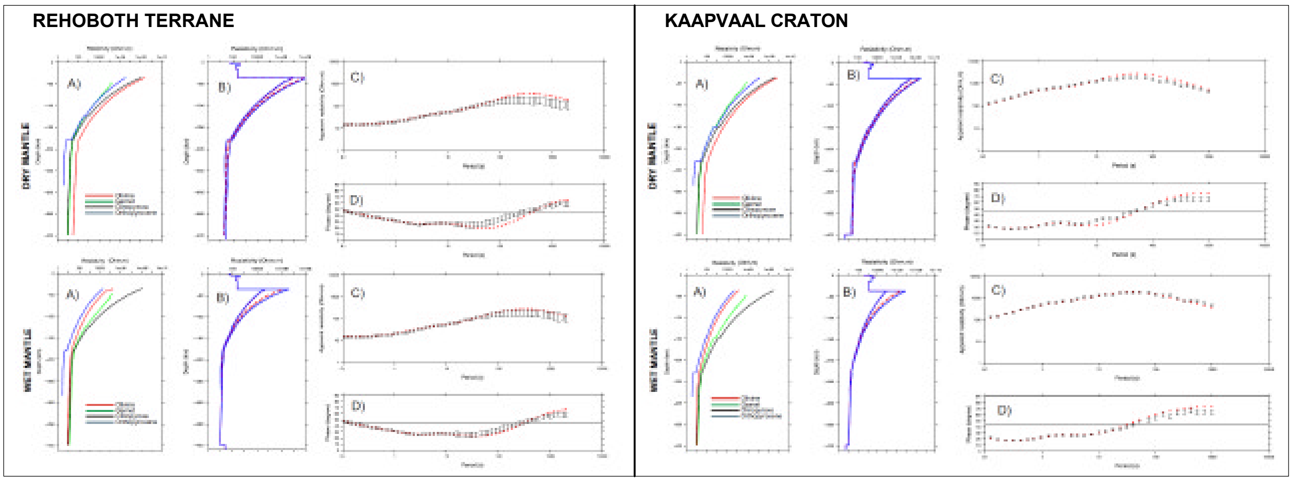

Figure 3. Modelled 1-D MT responses for the Rehoboth Terrane (site KIM426, Fig. 1) and Kaapvaal Craton (site KIM015). For the Rehoboth Terrane model: lithospheric thickness 180 km, with upper 80 km thick layer of low-T lherzolite (Table 1) and lower 60 km thick layer of high-T lherzolite. For the Kaapvaal Craton model: lithospheric thickness 220 km, with upper 100 km thick layer of harzburgite and lower 80 km thick layer of low-T lherzolite. Crustal thickness for both areas is 40 km. (A.) Electrical resistivity versus depth profiles for individual mantle mineral components, computed using LitMod. (B.) Resistivity depth profiles. In the mantle, the upper and lower Hashin-Shtrikman (1963) bounds (red dashed lines) are shown and the series (upper bound) and parallel (lower bound) averages (blue solid lines). The crustal resistivity structure for each terrane was derived using an Occam 1-D inversion of the "invariant" of the observed MT responses (i.e., geometric mean of rhoXY and rhoYX; arithmetic mean of phaseXY and phaseYX). (C.) and (D.) Predicted apparent resistivities and phases respectively for the lower Hashin-Shtrikman bound model (red diamonds) shown with respect to the observed MT data (black points with error bars that reflect the maximum of observational error and departure from a 1-D assumption). The upper row of figures corresponds with a dry mantle structure. The lower row represents a hydrous mantle, characterised by olive and orthopyroxene water contents of 40 ppm and 200 ppm respectively.